Hybrid solar-driven interfacial evaporation systems: Beyond water production towards high solar energy utilization

Tianpeng Ding [1], Yi Zhou [1], Wei Li Ong [1], Ghim Wei Ho [1,2,3,*]

[1] Department of Electrical and Computer Engineering, National University of Singapore, 4 Engineering Drive 3, Singapore 117583, Singapore
[2] Department of Materials Science and Engineering, National University of Singapore, 9 Engineering Drive 1, Singapore 117575, Singapore
[3] Institute of Materials Research and Engineering, A*STAR (Agency for Science, Technology and Research), 3 Research Link, Singapore 117602, Singapore

Owing to its promising approach to tackling freshwater scarcity, solar-driven interfacial evaporation (SDIE) which confines the photothermal heat at evaporating surface has attracted tremendous research attention. Optimizing efforts on photothermal conversion and thermal management have greatly improved the SDIE performance. By taking advantage of the heat localization strategy, hybrid SDIE systems have been designed to enhance the solar energy utilization beyond water production. In this review, the development of SDIE and energy flow in hybrid system are discussed. The advanced conceptual designs of different hybrid applications such as electricity generation, fuel production, salt collection, photodegradation and sterilization are comprehensively summarized. Moreover, the current challenges and future perspectives of the hybrid systems are emphasized. This article aims to provide a systematic review on the recent progresses in hybrid SDIE systems to inspire both fundamental and applied research in capitalizing the undervalued auxiliary energy sources for future integrated water, energy and environmental systems.

Keywords: Two-dimensional; Metallic nanocrystals; Renewable energy; Electrocatalysis

Introduction

Water shortage poses a growing threat to sustainable economic development and social progresses. The freshwater scarcity situation is exacerbated by the on-going population growth, climate changes and environmental pollution [1]. Although there is an abundant water on Earth, 97% is seawater, which is not suitable for direct drinking, domestic or industrial usage. Therefore, it is of great significance to develop efficient and large-scale desalination technologies to produce freshwater from seawater or even waste water. However, most of the existing desalination technologies such as reverse osmosis (RO) [2–5] and low-temperature multi-effect distillation (MED) [6,7] are implemented at great capital expense and high energy consumption, which are unfeasible for remote and off-grid regions. Consequently, addressing the contradiction between water purification and energy consumption becomes a critical issue for sustainable freshwater production.

Solar energy has been widely used since ancient times, and being an inexhaustible and environmentally friendly energy source, it continues to attract immense attention to provide a highly promising way to address numerous challenges [8–15]. Photothermal effect is a motivating force of the natural hydrologic cycle and atmospheric circulation, which also brings inspirations for tackling water scarcity issues [16–18]. Solar-driven water evaporation, which uses sunlight as the sole energy source to vaporize water through photothermal effect, circumvents the huge obstacles between freshwater supply and energy consumption. However, the traditional solar-driven evaporation systems usually have low yield due to poor light absorption efficiency and massive heat dissipation [19,20]. In this context,

* Corresponding author at: Department of Electrical and Computer Engineering, National University of Singapore, 4 Engineering Drive 3, Singapore 117583, Singapore.
E-mail address: Ho, G.W. (elehgw@nus.edu.sg)

  https://doi.org/10.1016/j.mattod.2020.10.022

researchers have spent considerable efforts to develop advanced and efficient solar vapor systems to take full advantage of the sunlight.

In recent years, a highly efficient solar-driven interfacial evaporation (SDIE) system [21–23] radically different from the common bulk [24] or volumetric [25–27] evaporation strategies was developed. The solar absorber is located at the water–air interface with confined water path to thermally insulate the absorber from the bulk water. With this, the photothermal heat is confined to the evaporating interface, where only a small volume of water is heated, while the underlying bulk water temperature remains largely unchanged, close to the ambient. Consequently, detrimental heat dissipation is largely suppressed and the temperature of light absorber is greatly increased, boosting evaporation efficiency to over 90% [28–33]. Besides affording minimal use of photothermal materials, such evaporating strategies also offer the flexibility to tune the vapor flux and vapor temperature, setting the stage for other applications beyond evaporation such as electricity generation [34–38], fuel production [39–41], salt collection [42–44], and so on. So far, there are many excellent and comprehensive reviews that systematically summarized the development of the SDIE systems, meanwhile, in-depth analyses of the materials and system designs that can improve the performance of water evaporation are made available [20,29,45–53]. These meaningful discussions will undoubtedly enlighten and advance the research in SDIE system. However, though many researchers have integrated various applications with the evaporating systems, existing review articles mainly focused on the photothermal materials and system designs that can improve evaporation efficiency, while these hybrid applications merely serve as complements with insufficient or incomprehensive discussions. To date, there are few, if any, articles focusing on important and mutually compatible applications beyond evaporation that are promising in managing the energy-water-environment nexus [8,20,54–56]. In view of this upcoming research area as mankind seek for better performing and multi-function integrated systems, it is necessary and timely to review the recent progresses and gain insights into this interdisciplinary research field to accelerate its development.

The goal of this review is to provide a systematic overview of the recent progresses in hybrid SDIE systems and the relevant advanced concepts that enrich the solar energy utilization. We first provide a comprehensive summary of the state-of-art development of the SDIE with advanced photothermal conversion and thermal management strategies. Next, the energy flow and the types of potential energy sources present in the SDIE system that can be capitalized for other applications will be discussed. We will then present an overview of the recent efforts on utilizing the undervalued energy sources in the SDIE. In terms of application, we classify them into two main types: (1) energy harvesting including electricity generation and fuel production; and (2) other applications including salt collection, photodegradation, sterilization, etc. Finally, we point out the opportunities and challenges of the hybrid applications in the SDIE systems. This review is aimed at providing an in-depth understanding of the various complementary approaches that can fully utilize the energy in a SDIE system, towards high-efficiency solar utilization, beyond freshwater production.

Development and energy distribution of the SDIE system

Development of the SDIE

As an emerging solar-driven freshwater collection technology, the unique local heating feature endows SDIE with more flexibility in tuning and optimizing the system. The water evaporation efficiency is mainly determined by two critical factors: (1) photothermal conversion capability which determines the total amount of energy the evaporation system can utilize, and (2) thermal management which shapes the energy flow in system to distribute the photothermal heat for water vaporization. Desired SDIE system can efficiently absorb and convert the sunlight into heat by photothermal effect, and maximally transform the heat to water vaporization.

Solar absorbers, as the media to convert solar radiation, play the primary and critical role in a SDIE system. In recent years, advancements in nanotechnology and nanoscience have brought vitality to photothermal materials to make full use of the broadband sunlight. To date, various types of photothermal materials have been investigated including plasmonic metals [21,57–62], semiconductors [63–70], carbon-based materials [71–78] and their hybrids [79,80].

Plasmonic metals: Plasmonic-based solar absorbers have demonstrated efficient photothermal conversion ability and already been extensively used in SDIE systems [60–62]. When the incident photon frequency match the inherent oscillation frequency of the free electrons within the metal surface, the plasmon-excited electrons generate with near-field enhancement and redistribute their energy through electron–electron scattering process, resulting in a light-to-heat conversion efficiency close to 100% [25,81]. So far, various kinds of metals such as gold, silver, aluminum, copper, cobalt etc. have been developed as plasmonic materials. [57,61,62,82,83] Gold [58,84] and silver [59,62] are the most commonly used plasmonic photothermal materials among them, owing to their superior plasmonic resonance properties and stability. As individual plasmonic nanoparticles can only absorb a narrow band of light around their resonance peak, nanoparticles with distributed sizes have been assembled together to achieve broadband light absorption. Moreover, assembly of metal nanoparticles can promote plasmon coupling causing the electric field at the interparticle gap to be enhanced by several orders of magnitude. However, the manipulation of particle size and subsequent assembling process increase the fabrication complexity and cost [45]. Other methods to tailor the position, broadness and intensity of the surface plasmon band can be achieved through dielectric properties of the surrounding medium, and Coulombic charge among the nanoparticles.

Semiconductors: Semiconductors have been widely used as solar absorbers because of their tailorable bandgap structures which lend themselves to be efficient solar to thermal conversion materials. Electron-hole pairs are excited by semiconductors when energy of incident light is higher than or equal to the bandgap, and then release the energy in the form of photons or phonons as the photoexcited electron-hole pairs return to low-level state [85]. However, most semiconductors have a wide bandgap with a narrow absorption wavelength and the released photons is detrimental to photothermal effect. To extend the absorption spectrum, band engineering is introduced to reconstruct and tune the bandgaps of semiconductors. For example, typical visible light transparent titanium dioxide (TiO_2) with a bandgap of 3.2 eV can only absorb UV light, while the reduced TiO_x turns to be black with whole solar spectrum absorption [63]. Recently, a series of broadband spectrum absorption semiconductors have been developed, including titanium-based semiconductors [63–65], CuS [66], $CuFeSe_2$ [67], NiO [68], Te [86], and so on. In addition, some emerging two dimensional (2D) semiconductors have also been used as photothermal materials, such as MoS_2 [69,87], Mxene [70] and black phosphorus [88,89]. Despite the huge potential in whole-spectrum photothermal candidates, semiconductor based absorbers often undergo complicated fabrication process and some of them, especially the chalcogenide semiconductors suffer poor stability in intense light irradiation and high temperature environment.

Carbon-based materials: Compared with the aforementioned plasmonic metals and semiconductor-based materials, the abundant sources, low cost, excellent processability and stability give the carbon-based materials superiority as photothermal materials. Additionally, the natural black property makes them particularly suitable for light absorption. Light heats the carbon-based materials through the thermal vibration of molecules involving the excitation of electrons and their subsequent relaxation [45]. To date, various kinds of carbon-based materials have been fabricated as superior candidates for solar absorbers, including carbon nanotubes (CNTs) [71–73], grapheme [76,77], graphene oxide (GO) [78], reduced graphene oxide (rGO) [90], carbon black [74,75], etc. Especially, carbonized materials from natural products not only provide more accessibility, but also further reduce the related cost [91–93]. As one of the most promising photothermal materials, the carbon-based materials should improve their mechanical strengths before large scale practical implementation, for example, the carbonized materials usually lose their compressive strength and flexibility.

Through elaborate design, solar absorbers synthesized with these photothermal materials can enable maximum absorption of solar energy over the whole solar spectrum via nanoscale plasmonic resonance, non-radiative relaxation of photoexcited electrons and thermal vibration of molecular or lattice. Besides the excellent photothermal materials, some structure-based designs can also contribute to the solar energy capture of the system, for example, 3D structure of absorbing surface can efficiently decrease the diffuse reflection energy loss through multi-scattering effect [62,94,95].

Although solar energy is absorbed and converted into heat by the absorber located at water–air interface, undesirable heat loss is still inevitable. Appropriate thermal management that localizes heat at the evaporating interface and suppresses heat loss plays a vital role in the resulting evaporation efficiency. The major heat loss occurs in two ways: downward conduction loss to underlying water body and upward convection and radiation losses to the environment. Tremendous efforts have been devoted to the design of advanced thermal management structure so as to minimize the unfavorable energy loss.

A straightforward way to reduce downward heat loss to water is to decrease the contact area between the heating absorber and underlying water body. Thermally insulating materials such as polystyrene foam can be sandwiched between the absorber and water to mitigate the downward thermal conduction, while 1D or 2D water channels are created to maintain a constant water supply for evaporation [96,97]. As a consequence, the conduction heat loss is suppressed owing to the reduced cross-sectional area of the water path. Some intrinsically porous materials, such as hydrogel and carbonized biomass, are ideal solar absorber candidates, because of their open-cell structure that not only facilitates water supply but also confines the water flow to suppress heat conduction [39,60,91].

In comparison with general evaporating strategies, the temperature of top evaporation surface in the SDIE system is much higher, which not only accelerates the vaporizing rate but also results in increased heat loss to environment via thermal convection and radiation. To diminish the convective heat loss, transparent polymeric bubble wrap has been used to cover the top evaporating surface to generate 100 °C steam under ambient air conditions without optical concentration [98]. Since heat convection and radiation rates are correlated with the surface temperature, lowering the surface temperature can reduce the heat loss to environment. The increase of the evaporating surface area through a pillar-structured design has shown to greatly decrease the temperature of side walls to be lower than the environment [99]. Such cooler surfaces harvest energy from the environment instead of transferring heat, resulting in evaporation efficiency over theoretical limit. Nevertheless, most inhibition of upward heat loss requires extra working space and possibly cause optical loss of the incident solar light.

Energy distribution in the system and potential energy sources

Solar-driven freshwater production is a complex and continuous energy transferring process with the sunlight as the original energy source. Fig. 1 shows the energy flow in a typical SDIE system, where incident sunlight is absorbed and converted into heat by photothermal materials. Majority of the photothermal heat vaporizes the water, thereby storing the photothermal energy in the form of latent heat [8,16,19,45]. Part of the absorbed energy is lost to the ambient through radiative and convective effects, and underlying water through conductive and radiative effects. As discussed previously, an elaborate design can maximize the energy used in vaporization and minimize the heat dissipation to environment or underlying water, so as to improve the evaporation efficiency. To complete the course of freshwater production, the generated hot vapor is subsequently diffused and condensed, accompanied by continuous latent heat release, to eventually harvest clean water.

Despite optimal utilization of sunlight for water vaporization, there is limited development on various untapped sources of energy present in the SDIE system for other possible applications. It is important to note that besides judicious choice of materials and strategic thermal management, a pragmatic use of the various energy sources can augment solar utilization efficiency. As a major energy consuming medium, hot vapor not only has high thermal energy but also high kinetic energy, capable of working directly as a heat source or convert into other forms of energy to drive a device mechanically or reactions chemically. In addition, the unique tiered construction of SDIE system, distinguished

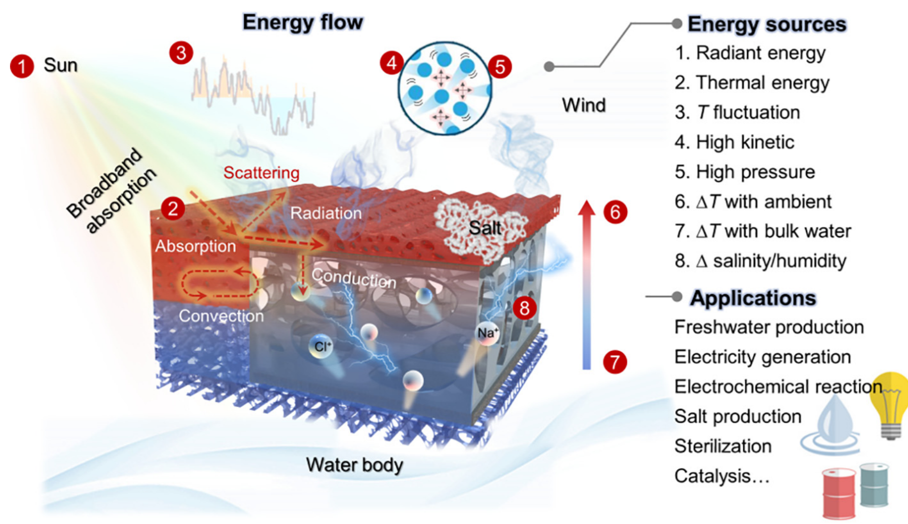

FIGURE 1

Schematic drawing of the energy transfer process and potential energy sources in the SDIE system.

from other evaporating system, is endowed with more potential energy sources. For instance, in a SDIE system, benefitting from the superior heat localization setting, the top evaporating surface has a much higher temperature than the environment and the underlying water body. These temperature differences subsume promising thermal energy that can be extracted. High temperature conditions existing in the system can also be used to improve the mass transport dynamics, such as accelerating the ions diffusion or carriers migration. Kinetic energy of the ions and carriers needed to overcome the enthalpy of migration barrier is largely increased with temperature. Taking advantage of these high temperature status, one can restore part of the dissipating heat and realize multiple tasks simultaneously. Moreover, when the water pumping path is reduced, ions diffusion is restricted, causing the salt concentration at the evaporating surface to be much higher than that in the bulk water. The entropy difference between the distinct salinity conditions is another promising means in electricity generation, of which the available energy density is theoretically six times larger than that between seawater and river water.

As a wide spectral range irradiation, solar energy covers a wavelength range of 300 nm to 2.5 μm. Though broadband light absorption and conversion of solar light to heat is favorable for the evaporation, indiscriminative conversion of light to heat across the full spectrum may hamper efforts to the optimization of a hybrid system. Special design that selectively harness photons of different wavelength will provide a more efficient solar energy utilization. Moreover, since SDIE system is targeted for natural sunlight implementation, especially in remote unstructured conditions, surrounding ambient, such as wind and tidal wave, also provide additional possibilities and availabilities to improve the overall system efficiency and meet specific demands. So far, various intricate designs have been proposed to make the utmost of the various energy sources. They not only enhance the solar utilization efficiency, but also direct at providing additional commodities, beyond freshwater.

Energy harvesting of hybrid SDIE system

Solar-driven water-electricity production

Recently, solar-driven water evaporation integrated with electricity generation has attracted tremendous attention, since it may provide renewable and decentralized clean water-electricity solutions especially useful for rural areas and developing countries [15,16,45,56]. In view of the energy flow for typical exclusive water evaporation schemes (Fig. 1), the photothermal heat is localized at the absorber and utilized for solar vaporization, while the internal enthalpy of water body and steam are usually lost to the environment, which restrains the overall solar energy utilization. Interestingly, other energy harvesters can be introduced into SDIE systems by rational design to serve multipurpose functions i.e. electricity generation, thermal insulation, heat scavenging, and vapor condensation, thus facilitating a synergistic enhancement of water evaporation and electricity generation. For instance, the heat confinement and localization of interfacial solar absorber in the SDIE system result in a temperature difference ($4 \sim 8\,°C$ for one-sun illumination) between liquid–air interface and underlying water [14,37,100,101], this low-grade heat is a promising energy source for waste energy-to-electricity harvesting.

In order to harvest the thermal energy between the absorber and underlying water body, Ho's group devised a thermoelectric generator (TEG) based hybrid water-electricity co-generation system, as shown in Fig. 2a [15]. Commercial Bi_2Te_3-based TEG serves as a thermal insulator under carbon-based absorber to promote water evaporation. The introduction of TEG isolates the carbon-based absorber from body water and reduces the downward heat conduction, thus enhanced the water evaporation rate from 1.2 (without TEG) to 1.36 kg $m^{-2}h^{-1}$ and concurrently realized output power density of 0.4 W/cm^2 under one-sun intensity. The commercial TEG used in this work not only ensures a high reliability/durability for off-grid applications but also provides a solution for cost-effective production of water and

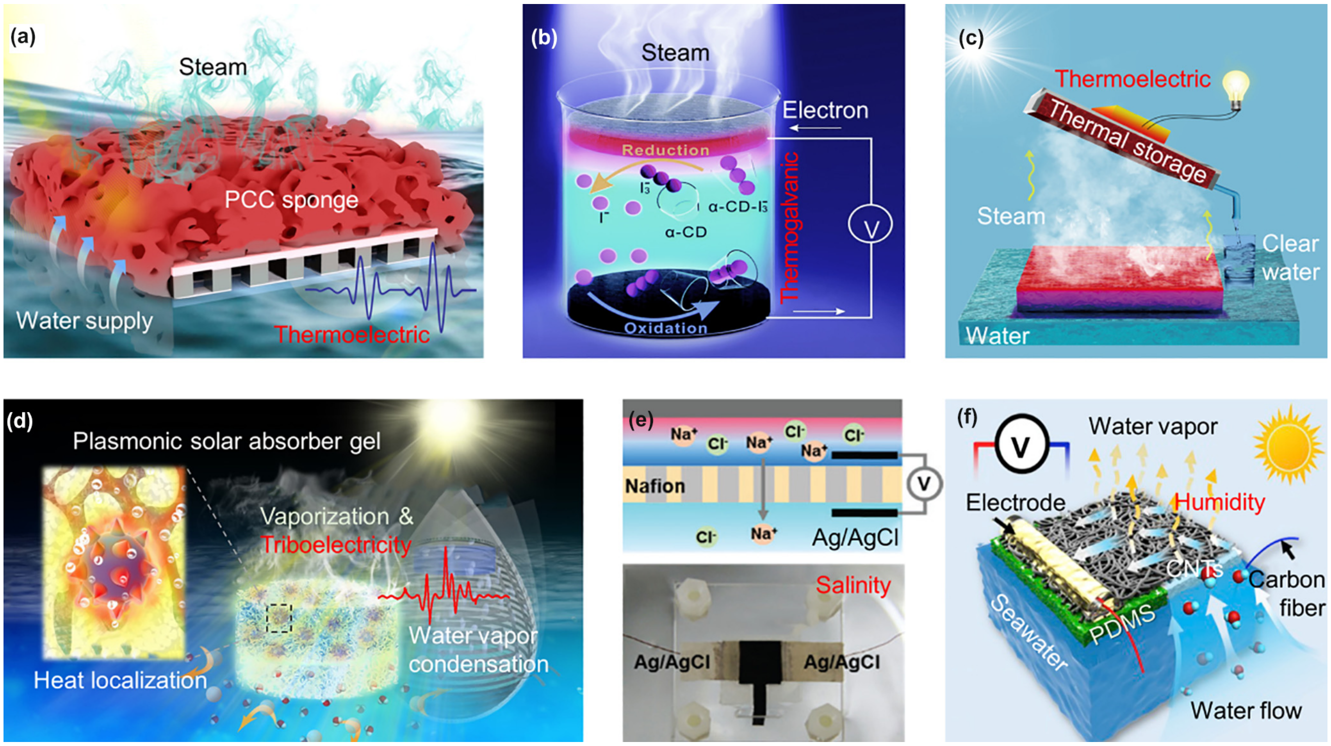

FIGURE 2

Solar-driven water evaporation and thermal energy harvesting. (a) TEG integrated with absorber and served as a thermal insulator to harvest the conductive heat [15]. (b) TGG with I_3^-/I^- and α-CD electrolyte for conductive heat utilization [35]. (c) TEG-enabled heat scavenges of water steam [34]. (d) TENG for scavenging the condensed droplet flowing by liquid–solid interfacial contact-separation [60]. (e) Simultaneously produce water and electricity by using CNT-based absorber and ionvoltaic salinity harvester [103]. (f) Water evaporation and capillarity-driven electricity generation based on hybrid wettability [104].

electricity. Beside the TEG-enabled solar-driven water-electricity co-generation, thermogalvanic/thermoelectrochemical techniques are also introduced to harvest the temperature difference between the liquid–vapor interface and underlying water [35,102]. In these designs, the redox couples are dissolved into the water body, two electrodes of thermogalvanic generator (TGG) are assembled onto the absorber and bottom of body water, the temperature-dependent electrochemical potential is generated by reduction–oxidation reactions occurred on the two electrodes, producing a steady output voltage. Deng's group integrated I_3^-/I^- redox couples into SDIE system and performed an open TGG for water-electricity co-production, as shown in Fig. 2b. Under one-sun illumination, the water evaporation rate of 1.1 kg $m^{-2}h^{-1}$ and power density of 0.5 mW/m^2 were achieved by using the TGG-integrated SDIE system, these results are higher than that of the water-electricity co-generation system without graphite felt. Compared to Bi_2Te_3-based TEG for waste heat harvesting, the I_3^-/I^--enabled TGG indicates a larger thermopower, attributed to the higher Seebeck coefficient. This design also provides a power density of 0.23 μW/m^2 under natural evaporative cooling without sunlight. Nonetheless, the electrolyte-based electrical conduction of TGG leads to a high inner resistance, which restricts the output power maximization (of the order of mW/m^2) in comparison with semiconductor-based TEG (of the order of W/m^2).

Aside from the low-grade waste heat harvesting between the solar absorber and underlying water, the internal enthalpy of kinetic hot vapor can also be scavenged into electricity. In theory, the temperature of steam released from the absorber can reach to ~100 °C by using optical engineering design. The amount of vapor as well as condensation latent heat can be enlarged with increased solar power illumination. In view of the storage and recovery of interfacial solar steam enthalpy, Zhu's group introduced a thermal storage layer integrated with Bi_2Te_3-based TEG to recover energy from the high-temperature steam and produce steady electrical output (Fig. 2c). The upward vapor generated by graphite/nonwoven solar evaporator film reaches the bottom surface of the thermal storage and condensates into water droplets by releasing latent heat. The temperature difference between the thermal storage and the environment is converted into electricity using TEG. In this work, the water evaporating rate of 34.8 kg $m^{-2}h^{-1}$ and electricity output of 574 mW are achieved under a simulated solar intensity of 30 kW/m^2, and an electronic fan is directly powered by the output electricity [34]. Additionally, not only the thermal energy but also the kinetic energy of steam can be scavenged, especially for water evaporation under unstructured airflow conditions. Ho's group demonstrated a ferroelectric fluoropolymer polyvinylidene fluoride (PVDF) cantilever to harvest the thermomechanical energy of vapour [105]. By coupling the pyroelectric and piezoelectric effects, highest power density of 0.24 mW/cm^2 is achieved via heating–cooling and mechanical oscillation of PVDF film during evaporation under one sun. Aside, simultaneous demonstration of vapor condensation which is the final step for truly water harvesting and exploitation of condensate water interfacial friction is rarely reported. Fig. 2d presents a solar absorber integrated with triboelectric energy harvester for simultaneous solar vaporization and electricity generation [60]. Hydrophobic polytetrafluoroethylene (PTFE) film was used for vapor condensation, and the large difference of triboelectric charge density between water and PTFE is ideal for triboelectricity [106]. The triboelectrification and charge contact-separation of water and PTFE leads to a maximum peak power output of 0.63 μW.

Also, the energy contained in the salinity difference of the solution between evaporation interface and underlying water body was harvested by Zhou's group through a Nafion selective membrane, as shown in Fig. 2e [103]. In theory, the amount of energy derived from mixing brine (5 mol/L) with river water (0.01 mol/L) per m^3 is around 16.9 MJ at room temperature (~20 °C) [107]. The low thermal conductivity ($0.1 \sim 0.2$ W m^{-1}-K^{-1}) of the Nafion membrane is beneficial for suppression of heat dissipation from the solar absorber to bulk water, thus leads to a high evaporation temperature and thermal efficiency. The high thermal efficiency enhances the water evaporation rate and results in a large salinity difference, thus facilitates ion diffusion and enlarged current under the same voltage. Consequently, this hybrid water-electricity system not only generates electricity but also recovers the heat loss of water body. The solar thermal efficiency of 75% and an ionvoltaic power density of 1 W/cm^2 are realized simultaneously under one sun illumination. Moreover, based upon the hybrid wettability and capillary-driven water supply, evaporation-induced humidity electricity generation is investigated in the past few years [108,109]. Assisted by solar water evaporation, hydrophobic PDMS, and hydrophilic CNTs film evaporator with distinct surface tension energy are designed to achieve water flow-induced energy harvesting (Fig. 2f). Under one sun intensity, the evaporation rate of 1.15 kg·m^{-2}·h^{-1} and output power of 2.1 μW are measured concurrently during the outdoor test [104].

Apart from direct waste heat harvesting, the non-heat enthalpy, evaporation-induced chemical potential, also boosts energy-efficiency of solar-driven water evaporation. Conventional approaches have delivered broad spectrum solar absorption ($500 \sim 2500$ nm) using plasmonic nanostructured metals, semiconductors and carbon-based materials as-mentioned previously [16]; while the non-heat photon energy recovery has not attracted much attention. Recently, PV cell for Joule heating towards enhanced water evaporation is reported by a rational combination of the photo-electro-thermal effect of grapheme [110]. In this work, the high evaporation rate of $2.01 \sim 2.61$ kg·m^{-2}·h^{-1} is achieved under one-sun intensity, by concurrent solar heating and PV-aided electrical heating of porous graphene sponge/graphene foil (PGS/GF) architecture (Fig. 3a). Compared with merely solar heat absorption, the integration of PV cell electrical heating facilitates enhanced water production rate by 4.5 times, which warrants a highly-efficient solar-driven evaporation system. Traditionally, the short-wavelength (above-bandgap) photons is captured by PV cell, while the relaxation of electrons excited by short-wavelength light and photothermal conversion caused by long-wavelength (below-bandgap) photons lead to self-heating of photovoltaics. This large amount of waste heat results in non-negligible intrinsic excitation of electrons and holes for semiconductor PV cells and thus deteriorates the electrical output. To optimize the thermal management in conjunction with synergistic utilization of short-/long-wavelength photons, multi-stage photovoltaic-membrane distillation devices, and water-proof interconnecting layered structures and thermal insulation are investigated (Fig. 3b-d) [111–113]. In these designs, the waste heat of the PV cell is considered as an energy source to heat the evaporator layer and promote water evaporation; conversely, the heat dissipation by solar-driven evaporative cooling guarantees the high energy efficiency of PV cell. Therefore, a high evaporation rate of 1.64 kg·m^{-2}·h^{-1} (photothermal efficiency of 126%) and power density of 115.5 W/m^2 are achieved by spectrally selective absorber and commercial polysilicon PV cells under one-sun intensity. This PV-integrated water-electricity co-generation not only facilitates enlarged electricity output attributed to PV cooling but also maintains a high water evaporation rate for clean water production.

Followed by the energy flow of water evaporation, the comparisons of various solar-driven water-electricity co-production systems from working mechanisms, integrated structure designs, synergistic effects, and potential applications are tabulated in Fig. 4. Typically, thermoelectric and photovoltaic present high power density (over 1 W/m^2) and reliability, due to well-matched energy profiles, integrated with evaporators/absorbers as well as highly-efficient commercial energy harvesters. These results are reflected in Table 1 as well, which is a summary of the evaporation and electricity generation performance of the various absorber/evaporator and energy harvesting materials reported in recent literatures. In view of heat dissipation and water flow-induced enthalpy fluctuation during the water evaporation process, the diversification of water-electricity production facilitates the enhancement of photothermal energy utilization assisted by materials innovation [104,114], structure design [108,115], and system integration [37,116,117]. A summary of various reported electrical power density (P_e) and water evaporation rate (m_w) are plotted in Fig. 5, revealing that the solar-driven water evaporation coupled with PV/TEG technologies is more promising than others for concurrent electricity generation.

Solar evaporation-enabled fuel generation

Other than electricity generation, non-fossil fuel production is always an important endeavor to reliably meet energy demand. The most direct and clean method to convert solar energy into fuel is solar-driven catalysis. At present, photocatalysis has been widely used to produce fuel to fulfill the increasing worldwide energy demand. However, its practical viability is hampered by some primary challenges including limited ultraviolet–visible solar light absorption and sluggish charge transfer dynamics [120]. Compared to the traditional light-driven photocatalytic process, the use of both light and heat (photothermal effect) is capable of extending the absorption range beyond the inherent optical bandgap and accelerating reaction kinetics to further enhance photochemical and/or thermochemical reactions [9,18]. One prevalent issue in a typical photochemical suspension system is the shielding effect of the upper suspending photocatalysts and light absorption/scattering of water, especially in the case of sedimentation [39]. The solar absorbers in a SDIE system can readily serve as anchor matrix, which will not only

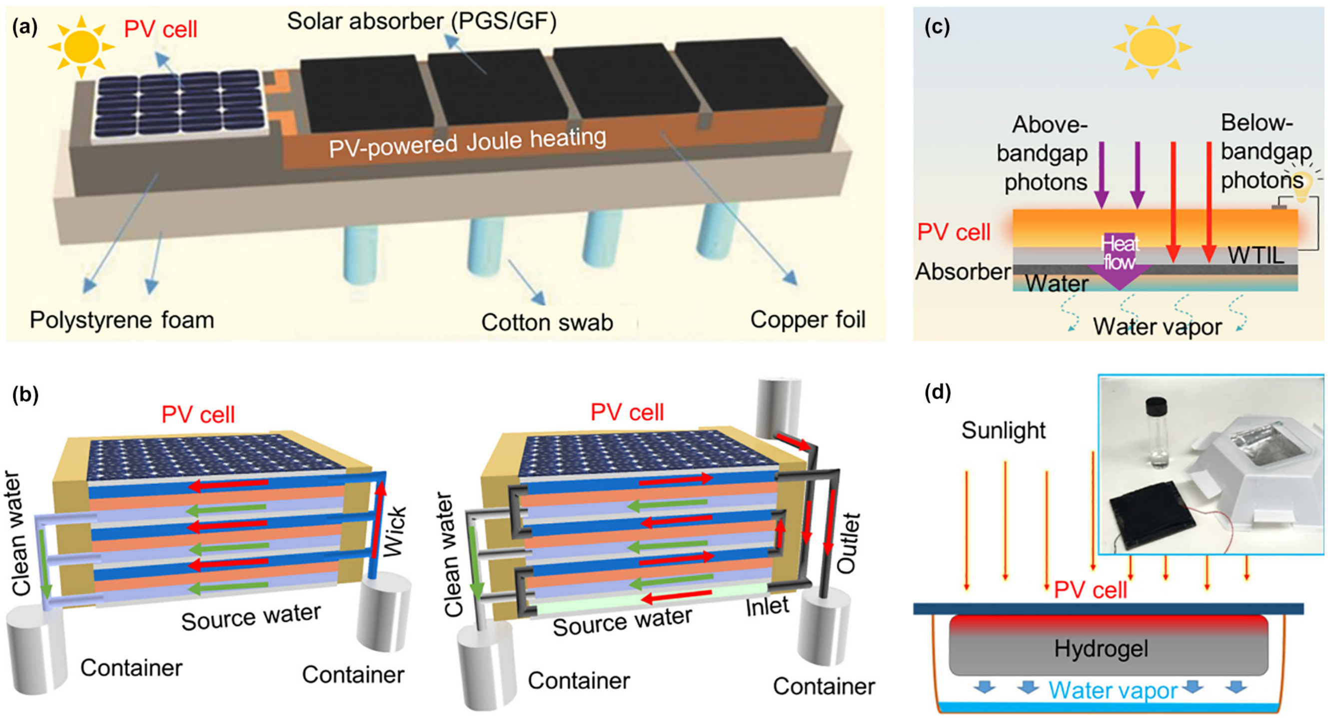

FIGURE 3

Solar-driven water evaporation and photon energy harvesting. (a) PV cell coupled with PGS/GF evaporator to co-generate electricity and water [110]. (b) Synergistic water-electricity generation achieved by water-cooled PV cell and evaporator membrane [111]. (c) PV cell with designed water-proof interconnecting layered structures for utilizing above-/below-bandgap photons, respectively [112]. (d) Hydrogel-based water desorption-absorption for PV cell cooling and enlarged electricity output [113].

circumvent the light penetration issue, but also greatly reduce the usage of photoactive materials and recycling difficulty. Thus, through rational design, photocatalysis fuel production and photothermal freshwater production can be achieved synergistically. In particular, some plasmonic-based photothermal materials such as gold, silver and platinum nanoparticles have found to facilitate the visible light utilization for photocatalytic fuel generation [16].

To this end, Ho's group proposed a photothermal catalytic gel to realize cogeneration of freshwater and hydrogen, as shown in Fig. 6a-b [39]. The gel consists of TiO_2/Ag nanofibers (NFs) and water absorber chitosan polymer, where the TiO_2 NFs act as photoredox materials and Ag nanoparticles play the role of plasmonic solar absorber and catalyst for enhanced charge transfer to improve hole-scavenging activity. It is worth noting that, its 3D gel framework provides excellent thermal management for SDIE, and at the same time immobilizes the catalysts and photothermal materials. By means of the vapor pressure gradient and a hydrophobic membrane, freshwater and hydrogen collection can be realized. And a solar vaporization rate of $\sim$1.49 kg m^{-2}h^{-1} and hydrogen generation rate of $\sim$3260 µmol m^{-2}h^{-1} under 1 sun were achieved by this hybrid system.

Besides, photothermal evaporation is also coupled with thermoelectric and electrocatalysis to facilitate the diversification of energy commodities e.g. electricity and green fuel. Recently, Ho's group has successfully integrated electricity generation and electrochemical hydrogen production into a SDIE system (Fig. 6c-e) [121]. Tailored hydrogels for contrasting evaporative cooling and solar absorption heating are integrated with Bi_2Te_3-based TE generators to efficiently convert waste heat into electricity and drive electrocatalytic water splitting. This prototype demonstrates synergistic solar-driven water-electricity-hydrogen generation.

Apart from hydrogen, solar-driven evaporation has also been used in producing other chemical fuels, such as ethanol, methane and diverse hydrocarbon fuels. With the same objective of meeting the energy demand especially for off-grid sites, Halas and co-workers demonstrated a solar-driven ethanol production from cellulosic feedstock (Fig. 7a) [40]. In this system, high yield steam is produced by illumination of light-absorbing nanoparticles. The solar-generated steam is then used to hydrolyze feedstock into sugars and purify ethanol in the final processing step. Grimes and co-workers also demonstrated carbon dioxide and water vapor conversion to methane and other hydrocarbons using nitrogen-doped titania nanotube arrays (Fig. 7b-c) [41]. The bandgap modified titania enables the absorption and utilization of the visible portion of solar spectrum, while dispersed cocatalyst nanoparticles adsorb and drive the redox process of the reactants. A hydrocarbon production rate of 111 ppm cm^{-2}h^{-1}, or $\sim$ 160 µL g^{-1}h^{-1} under one sun was obtained. These works not only offer alternatives for fuel generation but also open new avenues for carbon recycling using renewable sources.

Solar-driven fuel generation accompanied by steam generation has offered a greener and more sustainable pathway to meet energy demand. To date, many similar photochemical examples

Solar-driven water-electricity co-generation	Thermal (induced) energy harvesting					Photon energy
	TEG	TGG	PyEG/PEG	TENG	IVG	PV
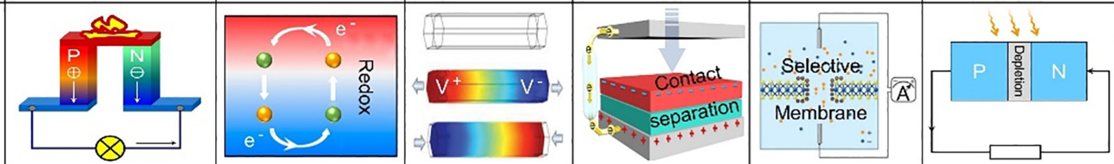						
Mechanism	Thermoelectric, Seebeck effect	Thermogalvanic, thermal diffusion	Pyroelectric, piezoelectric	Liquid-solid interface, triboelectric, electrostatic	Ionvoltaic, salinity, relative humidity	Photovoltaic, spectrum selective
Integrated structure with evaporator	Under absorber/ evaporator, above vapor	Under absorber/ evaporator, electrolyte in body water	Above vapor, cantilever	Below vapor, vapor/droplet condensation	Under absorber/ evaporator, ion selective membrane	Layered on evaporator (with interval)
Synergistical effects	Yes, thermal insulator	N/A	N/A	N/A	Yes, ion diffusion	Yes, PV cooling
Power density	High	Low	Low	High	High	Very high
Reliability	Very high	Low	High	High	Low	High
Output power management	DC/DC buck converter	DC/DC buck converter	AC/DC buck converter	AC-DC converter	DC/DC buck converter	DC/DC buck converter
Potential applications	Electrochemical production of hydrogen/bio-fuels, electronic/ thermal sensing, IoT	Electronic/ thermal sensing, IoT	Electronic/ thermal sensing	Electronic sensing, IoT	Salinity detection and analysis, electronic sensing, IoT	Electronic sensing, IoT, electrochemical production of hydrogen/ bio-fuels, IoT
References	[15,34,100]	[35, 102]	[105]	[60]	[103,109]	[110-112,118]

FIGURE 4

An up-to-date summary of the mechanism, integrated structure, synergistic effect, power density, and potential applications of various solar-driven water-electricity co-generation systems.

have also demonstrated, indicating manufacturing of commodity chemicals using natural sunlight is feasible, such as terebic acid, benzyl bromide and benzaldehyde [122–126]. Different from the usual predicament encountered by the solar-driven fuel generation that the conversion efficiencies are currently too low to justify industry investment, small-scale and decentralized fine chemicals manufacturing is of special applicability for natural sunlight utilization, such as flavor, fragrance and supplementary medicine (vitamins) industries [127]. Compared with traditional technologies, with the assistance of high temperature and vapor in the SDIE systems, solar-driven manufacturing fuels and other commodity chemicals is a more sustainable alternative approach that makes use of cost-efficient and sustainable energy sources.

Solar evaporation-driven multifunctional applications

Salt collection

In a SDIE system, salt concentration at the evaporating interface will increase and eventually precipitate on the solar absorber due to the suppression of ion diffusion. This will severely compromise the light absorption efficiency, leading to a gradual decrease in the water evaporation rate. Diverse salt fouling inhibition strategies such as backwash or chemical cleaning have been introduced [96,128–130], however, the concentrated solution after treatment, inevitably constitute to environmental harmful discharge of wastewater. Moreover, the precious mineral salts contained in the solution are wasted. Tremendous efforts have been devoted to solving these problems. Contrary to the prevention of salt sediment, intentional salt collection through proper strategies provides a novel approach to resource recovery [42–44].

Zhang and co-workers developed a novel solar steam generator composed of a horizontal evaporation dish and a vertical solution uptake thread, as shown in Fig. 8a-b [44]. Through controlled water transportation, edge-preferential crystallization and gravity-assisted salt harvesting, this SDIE system achieved continuous steam generation and salt collection in an uninterrupted long-term operation (over 600 h). Similarly, a paper-based SDIE system was designed to mediate a horizontal salt concentration gradient to establish a localized surface salt precipitation that

TABLE 1

Solar-driven water evaporation and electricity generation.

Photothermal energy utilization	Interfacial water evaporation				Energy harvesting		
	Absorber/ evaporator materials	Solar intensity (kW/m^2)	Evaporation rate ($kg\ m^{-2}h^{-1}$)	Photothermal efficiency (%)	Energy harvesting materials	Power density (W/m^2)	Refs.
Thermoelectric	PCC sponge	1	1.15	87.4 ~ 97	Bi_2Te_3	0.4	[15]
	CFW	1	1.26	81	Bi_2Te_3	0.4	[100]
	GN film	30	31.6	72.7	Bi_2Te_3	292.9	[34]
	CNP	1	0.92	58.6	Bi_2Te_3	0.22†	[37]
	Poly-NF	1	1.72	90	Bi_2Te_3	0.5†	[101]
Pyroelectric-piezoelectric	N_2-enriched carbon sponge	1	1.39	90	PVDF	240.7μ	[105]
Thermogalvanic	PDMS/CuO/Cu	1	1.33	91.4	Cu/Cu^{2+}	1.6 m	[102]
	Graphite felt	1	1.1	60	I_3^-/I^- pairs	~0.5 m	[35]
Triboelectric	Au Nanoflowers silica gel	1	1.36	85	Water/PTFE	0.16μ	[60]
Photovoltaic	PGS/GF	1	2.01 ~ 2.61	97.4	Silicon	200	[110]
	PTB7-Th	1	0.30	16 ~ 20	ST-PSCs	70.7	[118]
	SSA/Al	1	1.64	126	Polysilicon	115.5	[111]
	r-GO coated fiber	1	0.80	74.6	Polysilicon	204	[112]
Ionvoltaic	CNT modified filter paper	1	1.1 ~ 1.15	75	Nafion membrane (Ag/AgCl)	1	[103]
	CNTs film	1	1.15	/	CNT/PDMS paper	0.483 m	[104]
	Graphene/carbon cloth	1	1.3	83	Porous airlaid paper	0.37‡	[119]

Poly[4,8-bis[5-(2-ethylhexyl)2-thienyl]benzo[1,2-b:4,5-b′]dithiophene-alt-(4-(2-ethylhexyl)-3-fluorothieno[3,4-b]thiophene)-2-carboxylate-2,6-diyl]] (PTB7-Th); semitransparent polymer solar cells (ST-PSCs); spectrally selective absorber (SSA); reduced graphene oxide (r-GO).

† Solar absorber/evaporator for separate solar-driven water evaporation and electricity generation.

‡ Stands for the voltage.

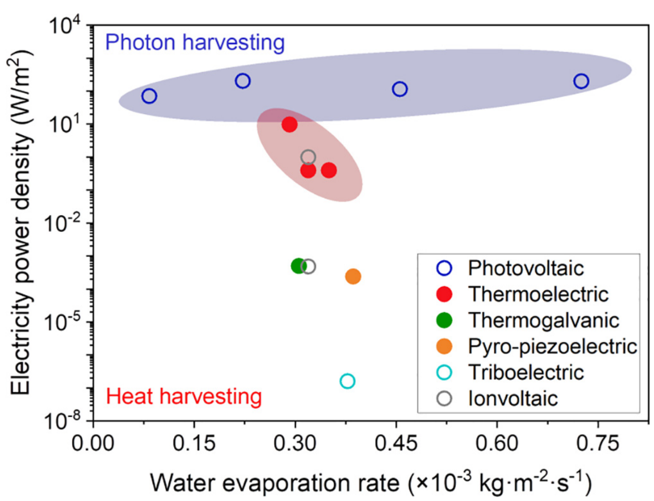

FIGURE 5

Reported data of water evaporation rate and electricity power density for illustrating the synergistic effect of solar-driven all-in-one water-electricity co-production. Thermoelectric [15,34,100], pyro-piezoelectric [105], thermogalvanic [35,102], triboelectric [60], photovoltaic [110–112,118], ionvoltaic [103,104].

successfully minimizes salt fouling and achieves concurrent salt extraction (Fig. 8c-e) [42]. This desalination system is capable of generating drinkable water out of 10 wt% brine with a solar-to-water conversion efficiency of more than 40% and NaCl of 0.42 kg m^{-2} per day. Besides increasing the salt productivity over traditional bulk heating solar salt production technology, it also avoids the multi-step treatments required in salt farms. Beyond NaCl salt, this technology also holds a remarkable potential to offer a new way of extracting other minerals, such as $MgCl_2$ and heavy metals, from seawater or industrial wastewater.

Photodegradation

Apart from the geographical and temporal uneven water distribution, water pollution is another critical factor that causes freshwater scarcity, especially in the industrial areas. Additionally, volatile organic components originating from human-activities and naturally occurring chemical compounds may be present in water sources will evaporate along with the water due to their low boiling point, causing contaminants in the water production. Photocatalytic technology has been considered as an environmentally friendly and cost-effective solution to remediate environment in the past decades. However, the far-flung and widespread nature of pollutants has increased the difficulties of photodegradation. Effective recycling of photocatalysts and efficient degradation rate are also requisite in commercial photodegradation application. Noticeably, the adsorption and concentration properties of the photo absorber during water evaporation are promising to address above mentioned problems [131]. Moreover, the localized heat at the catalytic sites can also improve the photodegradation efficiency. Combining photocatalysis and photothermal evaporation can be a multi-prong approach to solving the freshwater shortage [80,132–136].

A spectrum-tailored solar harnessing aerogel inspired by the spectrally selective sunlight utilization of plants was designed (Fig. 9a-b) [120]. The aerogel composed of oxygen vacancy (O_v) defect-rich semiconductor HNb_3O_8 (D-HNb_3O_8) nanosheets and polyacrylamide framework to perform water evaporation

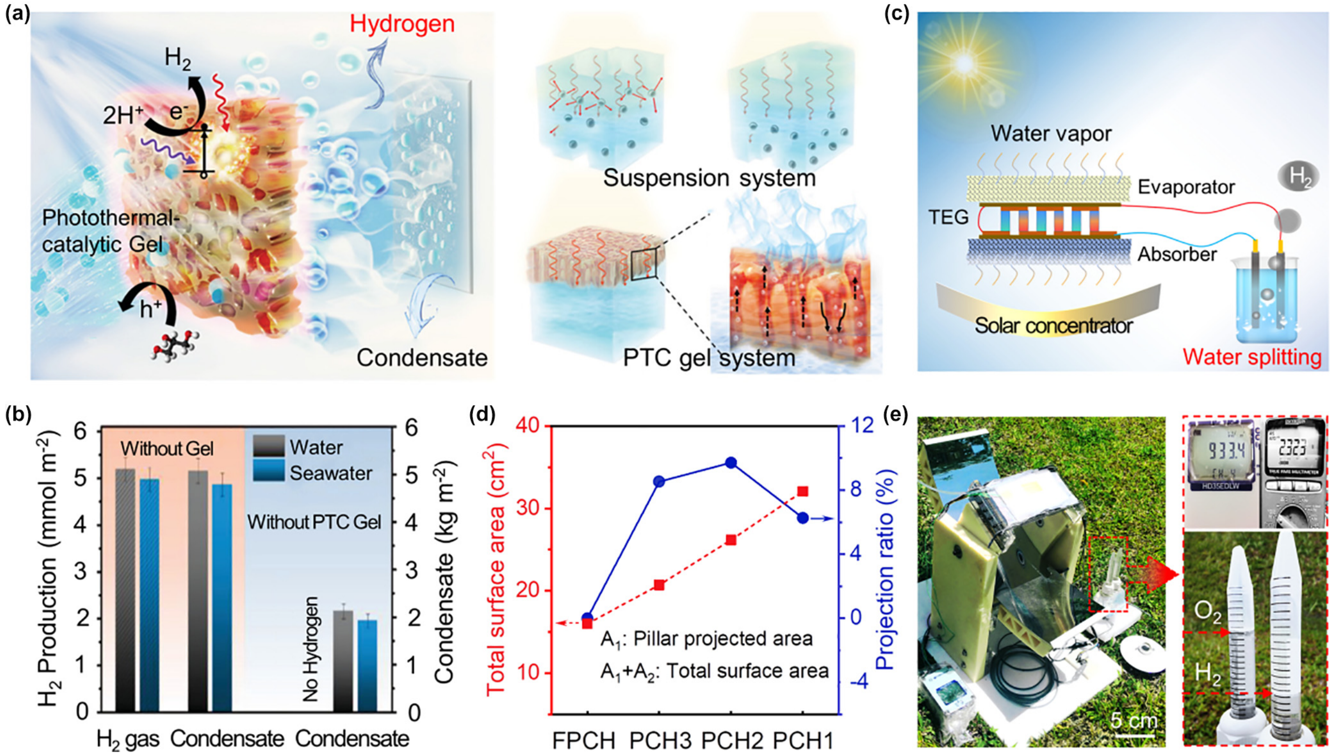

FIGURE 6

Hydrogen generation in SDIE systems. (a) Schematic drawing of the designed PTC gel for concurrent solar vaporization and hydrogen generation. (b) Hydrogen produced and condensate collected with and without the PTC gel under Xe lamp irradiation [39]. (c) Schematic for the synergistic hydrogen generation using TE modules. (d) Total surface area and projection ratio with different pillar dimensions (e) Digital photo of the set-up for outdoor testing [121].

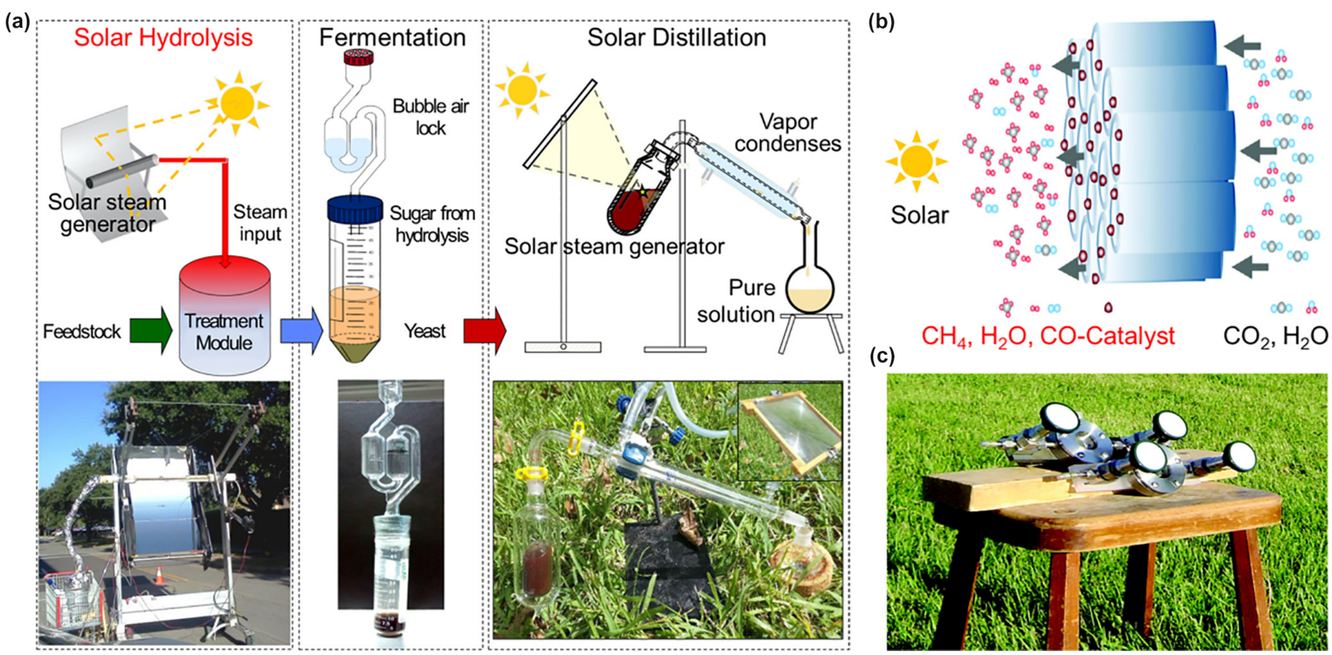

FIGURE 7

(a) Schematic representation and photographs of solar biofuel three-step process [40]. (b) Depiction of sunlight-driven photocatalytic carbon dioxide conversion to hydrocarbon fuels. (c) Digital photograph of the reaction chambers [41].

and photodegradation of organic contaminant. The aerogel selectively utilizes the whole solar spectrum, in which high energy ultraviolet photon is converted into high redox potential electron-hole pairs, while low energy visible-near infrared photon is transformed into heat. The introduction of heat to photodegradation greatly promotes the photochemical conversion

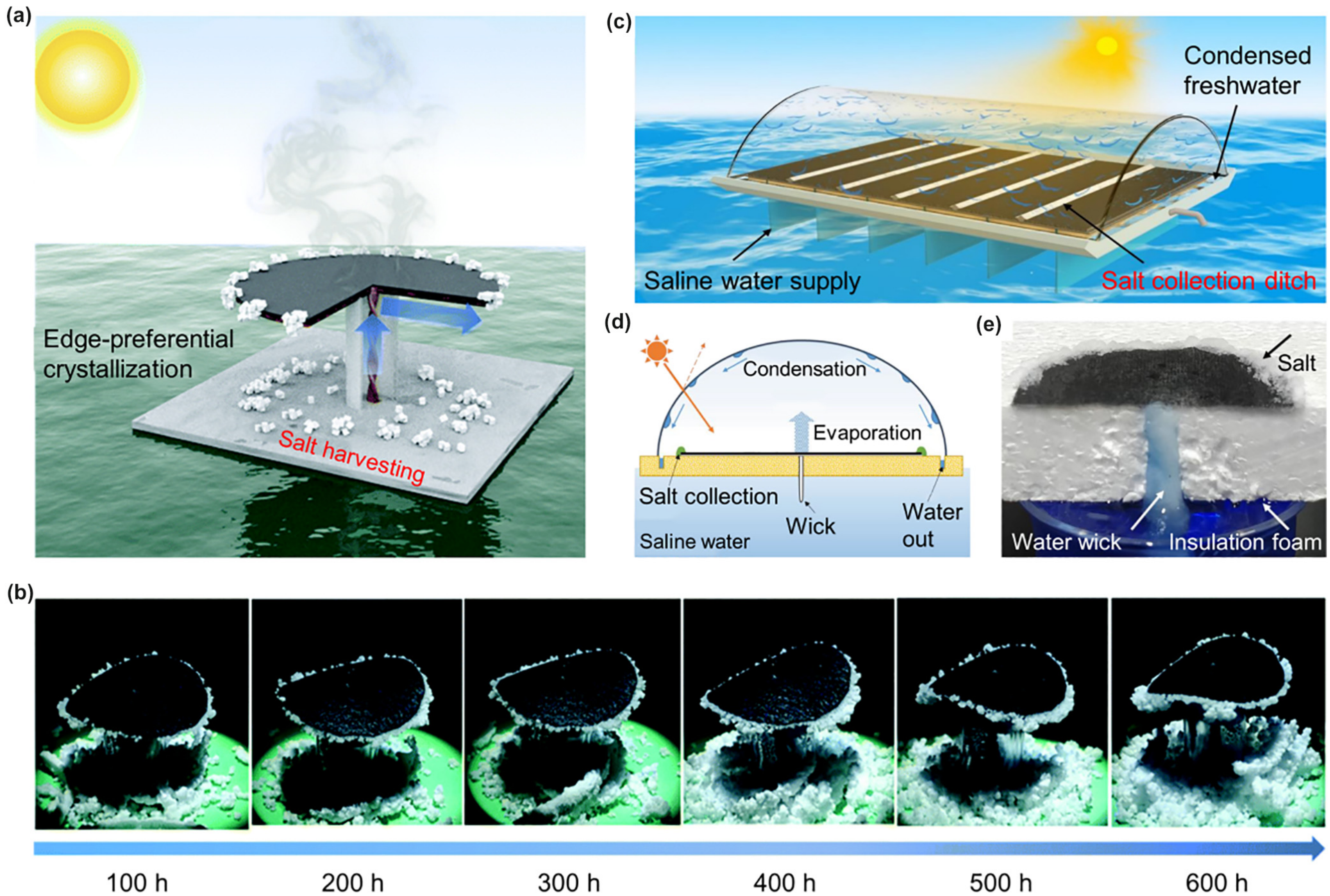

FIGURE 8

(a) Schematic illustration of the spatially isolated solar steam generation and salt harvesting. (b) Photographs of the salt harvesting performance during 600 hours [44]. (c) Schematic of the simultaneous freshwater and salt generation device. (d-e) Mechanism for the solar-driven interfacial desalination structure with localized surface salt precipitation design [42].

by providing high kinetic energy to the photogenerated electron-hole pairs and the reactants [61,137]. This in turn improves the charge carrier mobility, inhibit their recombination and increase the number of energetic interactions. Other than superior water evaporation performance, photoactivity enhancement is observed for the aerogel as rhodamine B is fully oxidized within 100 min, about 71% and 64% higher than that of the pure water and polyacrylamide aerogel. Another work, a synchronous solar distillation and photodegradation technology based on ZnO/-gold particles decorated membrane has been fabricated [133]. Steam generation rate reached $\sim 8.70\ kg\ m^{-2}h^{-1}$ and the concentration of organic pollutant (rhodamine B) in the residual water was reduced by ~ 70% within two hours of solar irradiation. Benefitting from the photochemical activity of TiO_2, Cai and co-workers designed an bifunctional fabric with photothermal effect and photocatalysis for highly efficient clean water generation (Fig. 9c) [138]. Besides the high solar evaporation rate of $1.55\ kg\ m^{-2}h^{-1}$, the designed TiO_2-PDA/PPy/cotton also present a photocatalysis with ~ 96% degradation of methyl orange (MO) under simulated solar irradiation over 3 h. Moreover, by introducing photocatalysis into the SDIE systems, solar absorber fouling issue is relieved to some extent.

Sterilization

Pathogenic bacteria contamination in water has been a great threat to the public health and steam sterilization has been widely used as one of the most effective sterilization methods. However, traditional steam sterilization mainly relies on electricity, which is unavailable or affordable under certain circumstance, especially for the undeveloped and off-grid regions where commercially available sterilization equipment is lacking or inoperable [139–141]. Sterilization can be realized alongside the high-temperature steam generated during the SDIE process. Notably, photothermal sterilization is an economical and green approach to deactivate bacteria and viruses in drinking water, devoid of by-product, which is especially suitable for decentralized household application.

To this end, Deng's group proposed a reduced graphene oxide/polytetrafluoroethylene composite membrane based SDIE system, which generates steam over 120 °C, demonstrating excellent sterilization capability [142]. Zhu's group also proposed a proof-of-concept sterilization system, solar autoclave, which is low-cost and operates with minimum carbon footprint [143]. Effective sterilization of ~99.999999% inactivation of pathogen is verified by both bacterial vegetative cells and spores test. To

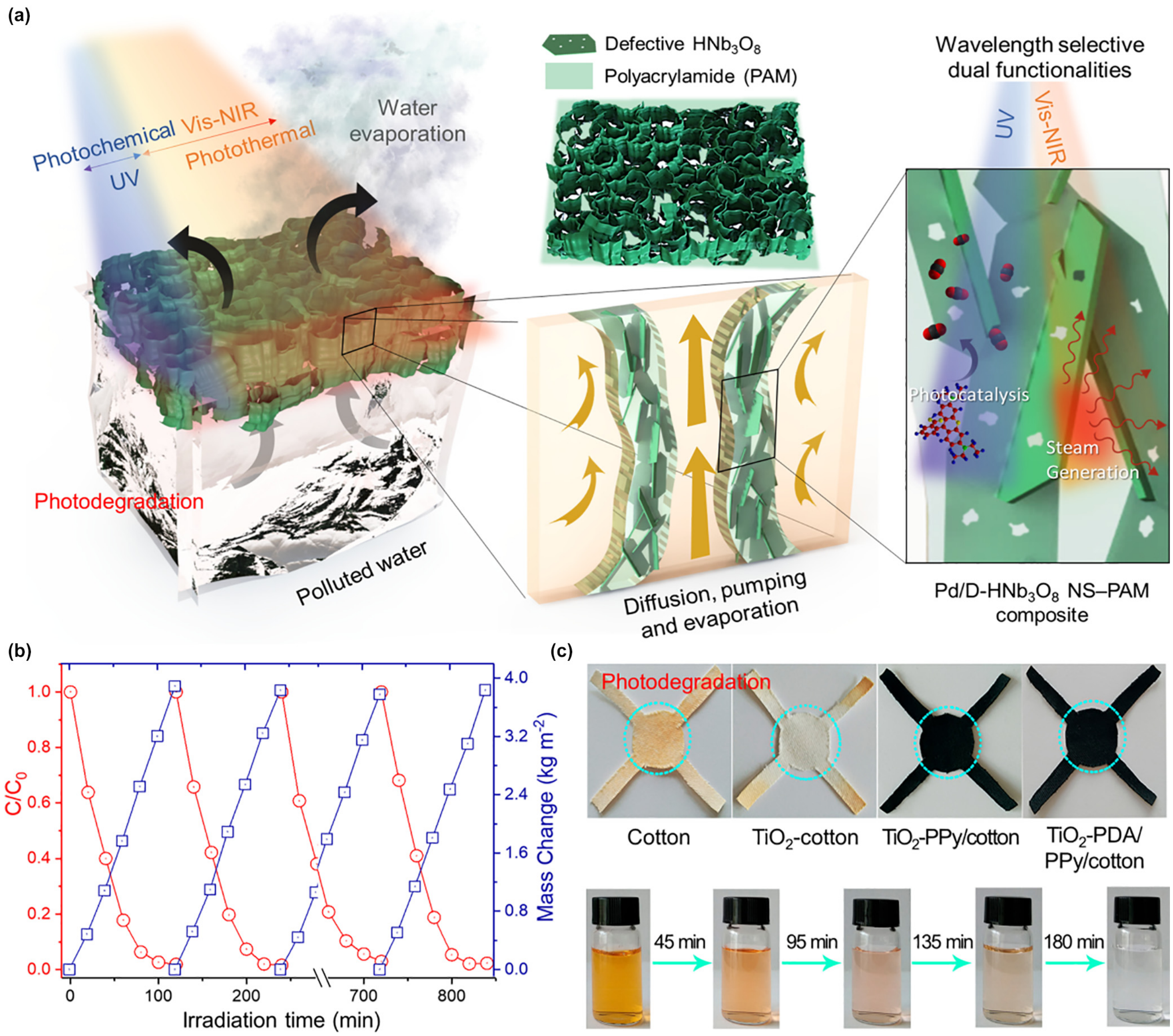

FIGURE 9

(a) Illustration of the synchronous photothermal and photochemical solar conversion of a defective D-HNb_3O_8/PAM aerogel. (b) Stability of the D-HNb_3O_8/PAM aerogel for photochemical oxidation and photothermal steam generation [120]. (c) Photodegradation performance for the TiO_2-PDA/PPy/cotton [138].

better facilitate the solar steam sterilization, a SDIE system is integrated into a portable solar vacuum tube [144]. Such portable solar steam sterilization generates high-temperature steam under ambient solar illumination and shows excellent sterilization of both geobacillus stearothermophilus biological indicator and escherichia coli bacteria. Besides, by taking full advantage of the high-energy region of the solar spectrum, disinfection capabilities of Ag_3PO_4-rGO photothermal textile through denaturation or oxidation of the bacteria biomolecules was demonstrated [131]. These solar steam sterilization technologies provide a low-cost solution to meet sterilization needs in undeveloped regions where electricity is lacking but solar radiation is ample.

Conclusion and perspective

With the rapid development of SDIE, various applications have been devised to couple with the freshwater collection systems to expand their functions and improve the overall solar utilization efficiency. In this review, key factors of the SDIE system namely photothermal conversion and thermal management are discussed. By analyzing the energy flow from sunlight absorption to vapor condensation during freshwater production, potential energy sources that come along with the system are discussed. These energy sources can then be harvested through rational and efficient designs for various additional functions which are broadly classified into energy and non-energy generation applications. We account the energy generation undertakings by reviewing various electricity and fuel harvesting strategies. Alternative applications including salt collection, photodegradation and sterilization are other feasible approaches for energy utilization, demonstrating the great potential of hybrid SDIE to interlink the water, energy and environmental nexus towards sustainable solutions. However, despite the perceived advantages and considerable achievements, all of the applications are largely in the conceptual stage. There remain challenges that need to be addressed before the commercial implementation at large scale.

Scientific standards for evaluating overall efficiency

As an emerging technology, standardized measurements and evaluation for the efficiency of a SDIE system are still lacking. Consequently, quantitative evaluation of the efficiency of a hybrid system becomes more difficult to assess. Moreover, different applications often closely linked/associated to other energy sources, and not merely solar energy. For example, the electricity generating performance in a TEG hybridized evaporation system is actually determined by the temperature of environment or other heat sinks. These added energy sources further complicate the efficiency calculation. Moreover, accurate assessment of the energy possessed by the productions is also challenging. Hence, it is imperative to establish scientific standards to guide future developments towards effective solar energy utilization.

In-depth understanding of the energy flow

Though many strategies have been proposed to harvest different energy forms in a SDIE system, lack of an in-depth understanding on the energy flow in the system has been an obstacle to maximize the exploitation of the energy. Further understanding of the energy flow in the system is favorable to optimizing not only the thermal management and evaporation efficiency, but also the designs of other applications. The energy originating from the SDIE system may flow via different processes and pathways, transferring from one medium to another and undergoing transformation along the way. Moreover, there are difficulties in quantifying, tracing and tracking the system energy when they are existing in different representations during the energy transformation process. Modeling and simulation of energy flow may be employed to understand and predict the performance of individual components and overall system. The added raw materials and output productions will greatly increase the types of forms of energy and complicate the system energy flow, such as the solar-driven fuel generation from different precursors.

Long-term stability in real conditions

Because of the real outdoor conditions can sometimes be harsh or extreme such as high humidity, high salinity, elevated temperature and heavy contamination, which then adversely cause the system performance to decline or even fail. Therefore, long-term stability of materials and device is paramount to the success of practical applications. A common issue that often occurs for electronics is the high humidity that stems from the evaporation, which is fatal for their proper functioning. Hence, it is necessary to design rational hybrid structure and system to ensure all the components work well for extended period.

Specially designed materials and devices for SDIE

Though different strategies have been designed to make use of the different types of energy to complement solar evaporation, the materials or devices adopted for the multiple applications in most of the devices are not well-designed or customized for the hybrid systems. As a result, the systems are not able to reach their fullest potential. The materials used and system configuration are to be designed to best suit the local available resources and community needs. Various optimization that may be analyzed include size, capital cost, lifetime, operating and maintenance of various components of the system. In the context of more than one production, effective and efficient separation and purification of each production is crucial for a hybrid SDIE system. As a cost-effective and eco-friendly technology that utilizes nature sunlight as energy source, SDIE is preferentially considered to be hybridized with the small-scale and decentralized application, possibly for rural and semi-urban regions where conventional grid supplies are not available or affordable. Applications that harness environmental energy and work at moderate temperature pressure, humidity etc. conditions are technically and environmentally viable to be integrated with the SDIE. Innovative and specialized materials, devices, concepts as well as new mechanisms, will have the potential to make the most out of the energy so as to improve the overall efficiency of the system.

Declaration of Competing Interest

The authors declare that they have no known competing financial interests or personal relationships that could have appeared to influence the work reported in this paper.

Acknowledgments

This research is supported by the Ministry of Education, Singapore, under its Academic Research Fund Tier 2 (Award MOE2017-T2-1-140 and MOE2017-T2-2-102).

References

[1] R.F. Service, Science 313 (5790) (2006) 1088.
[2] R. Wang et al., J. Membr. Sci. 355 (1–2) (2010) 158.
[3] C.Y. Tang et al., J. Membr. Sci. 354 (1–2) (2010) 123.
[4] M. Elimelech, W.A. Phillip, Science 333 (6043) (2011) 712.
[5] L. Malaeb, G.M. Ayoub, Desalination 267 (1) (2011) 1.
[6] A.D. Khawaji et al., Desalination 221 (1–3) (2008) 47.
[7] H. Wang, Nat. Nanotechnol. 13 (4) (2018) 273.
[8] P.J.J. Alvarez et al., Nat. Nanotechnol. 13 (8) (2018) 634.
[9] M.Q. Yang et al., Adv. Mater. (2018) 1802894, https://doi.org/10.1002/adma.201802894.
[10] L.A. Weinstein et al., Joule 2 (5) (2018) 962.
[11] G. Hodes, Science 342 (6156) (2013) 317.
[12] A. Shah et al., Science 285 (5428) (1999) 692.
[13] J. Gong et al., Chem. Soc. Rev. 48 (7) (2019) 1862.
[14] T. Ding et al., Adv. Energy Mater. 8 (33) (2018) 1802397.
[15] L. Zhu et al., Adv. Energy Mater. 9 (22) (2019) 1900250.
[16] M. Gao et al., Energy Environ. Sci. 12 (3) (2019) 841.
[17] L. Zhu et al., Nano Energy 57 (2019) 507.
[18] C. Zhang et al., Adv Sci (Weinh) 6 (18) (2019) 1900883.
[19] C. Chen et al., Joule 3 (3) (2019) 683.
[20] V.-D. Dao et al., Nano Energy 68 (2020) 104324.
[21] Z. Wang et al., Small 10 (16) (2014) 3234.
[22] H. Ghasemi et al., Nat. Commun. 5 (2014) 4449.
[23] L. Zhou et al., Nat. Photonics 10 (6) (2016) 393.
[24] A.E. Kabeel, S.A. El-Agouz, Desalination 276 (1–3) (2011) 1.
[25] O. Neumann et al., ACS Nano 7 (1) (2013) 42.
[26] O. Mahian et al., Int. J. Heat Mass Transf. 57 (2) (2013) 582.
[27] G. Ni et al., Nano Energy 17 (2015) 290.
[28] Y. Zeng et al., Energy Environ. Sci. 4 (10) (2011) 4074.
[29] J. Zhou et al., Adv. Funct. Mater. (2019).
[30] C. Tu et al., Small 15 (37) (2019) e1902070.
[31] Y. Sui et al., J. Mater. Sci. 55 (1) (2019) 298.
[32] H. Liang et al., Angew. Chem. Int. Ed. Engl. (2019).
[33] Y. Guo et al., Nano Lett. 19 (4) (2019) 2530.
[34] X. Li et al., Joule 2 (11) (2018) 2477.
[35] Q. Shen et al., J. Mater. Chem. A 7 (11) (2019) 6514.
[36] L.L. Zhu et al., Adv. Energy Mater. 8 (16) (2018).

[37] X. Zhang et al., Nano Energy 48 (2018) 481.
[38] W. Wang et al., Nat. Commun. 10 (1) (2019) 3012.
[39] M. Gao et al., Adv. Energy Mater. 10 (23) (2020).
[40] O. Neumann et al., ACS Energy Lett. 2 (1) (2016) 8.
[41] O.K. Varghese et al., Nano Lett. 9 (2) (2009) 731.
[42] J. Xu et al., Desalination 484 (2020).
[43] Y. Shao et al., EcoMat 2 (1) (2020) e12018.
[44] Y. Xia et al., Energy Environ. Sci. 12 (6) (2019) 1840.
[45] P. Tao et al., Nat. Energy 3 (12) (2018) 1031.
[46] X. Jin et al., ACS Appl. Energy Mater. 2 (9) (2019) 6112.
[47] F. Tao et al., Appl. Mater. Today 17 (2019) 45.
[48] Y. Pang et al., ACS Energy Lett. 5 (2) (2020) 437.
[49] Z. Xie et al., Adv Sci (Weinh) 7 (5) (2020) 1902236.
[50] Y. Lin et al., J. Mater. Chem. A 7 (33) (2019) 19203.
[51] S. Cao et al., J. Mater. Chem. A 7 (42) (2019) 24092.
[52] V. Kashyap, H. Ghasemi, J. Mater. Chem. A 8 (15) (2020) 7035.
[53] X. Wu et al., Mater. Today Energy 12 (2019) 277.
[54] L. Zhou et al., Natl. Sci. Rev. 6 (3) (2019) 562.
[55] Z. Wang et al., Sci. Adv. 5 (7) (2019) eaax0763.
[56] G. Liu et al., J. Mater. Chem. A 8 (2) (2020) 513.
[57] A. Lalisse et al., J. Phys. Chem. C 119 (45) (2015) 25518.
[58] L. Zhou et al., Sci. Adv. 2 (4) (2016) e1501227.
[59] N. Zhang et al., J. Mater. Chem. A 5 (40) (2017) 21570.
[60] M. Gao et al., Adv. Energy Mater. 8 (25) (2018) 1800711.
[61] M. Gao et al., Energy Environ. Sci. 9 (10) (2016) 3151.
[62] M. Zhu et al., Adv. Energy Mater. 8 (4) (2018).
[63] G. Zhu et al., ACS Appl. Mater. Interfaces 8 (46) (2016) 31716.
[64] J. Wang et al., Adv. Mater. 29 (3) (2017).
[65] M. Ye et al., Adv. Energy Mater. 7 (4) (2017).
[66] X. Wu et al., Nano Energy 56 (2019) 708.
[67] H. Liu et al., J. Mater. Chem. A 6 (39) (2018) 18839.
[68] H. Liu et al., Nano Energy 42 (2017) 115.
[69] D. Ghim et al., Nano Energy 53 (2018) 949.
[70] R. Li et al., ACS Nano 11 (4) (2017) 3752.
[71] Y. Wang et al., ACS Sustainable Chem. Eng. 4 (3) (2016) 1223.
[72] C. Chen et al., Adv. Mater. 29 (30) (2017).
[73] Y. Li et al., Adv. Mater. 29 (26) (2017).
[74] Y. Liu et al., ACS Appl. Mater. Interfaces 7 (24) (2015) 13645.
[75] P.D. Dongare et al., Proc. Natl. Acad. Sci. USA 114 (27) (2017) 6936.
[76] P. Zhang et al., ACS Nano 11 (5) (2017) 5087.
[77] Y. Ito et al., Adv. Mater. 27 (29) (2015) 4302.
[78] K.K. Liu et al., ACS Appl. Mater. Interfaces 9 (8) (2017) 7675.
[79] A. Politano et al., Adv. Mater. 29 (2) (2017).
[80] Y. Yang et al., Mater. Horiz. 5 (6) (2018) 1143.
[81] M.T. Sheldon et al., Science 346 (6211) (2014) 828.
[82] P. Fan et al., Nanoscale 8 (30) (2016) 14617.
[83] A.D. Rakic et al., Appl. Opt. 37 (22) (1998) 5271.
[84] Y. Liu et al., J. Mater. Chem. A 7 (6) (2019) 2581.
[85] C.M. Hessel et al., Nano Lett. 11 (6) (2011) 2560.
[86] C. Ma et al., Sci. Adv. 4 (8) (2018) eaas9894.
[87] X. Yang et al., Adv. Funct. Mater. 28 (3) (2018).
[88] Z. Sun et al., Angew. Chem. Int. Ed. Engl. 54 (39) (2015) 11526.
[89] W. Chen et al., Adv. Mater. 29 (5) (2017) 1603864.
[90] Q. Jiang et al., Adv. Mater. 28 (42) (2016) 9400.
[91] G. Xue et al., ACS Appl. Mater. Interfaces 9 (17) (2017) 15052.
[92] N. Xu et al., Adv. Mater. 29 (28) (2017).
[93] C. Jia et al., Joule 1 (3) (2017) 588.
[94] K. Li et al., Adv. Energy Mater. 9 (34) (2019).
[95] Y. Shi et al., Joule 2 (6) (2018) 1171.
[96] P.-F. Liu et al., Mater. Today Energy 8 (2018) 166.
[97] Y. Li et al., Nano Energy 41 (2017) 201.
[98] G. Ni et al., Nat. Energy 1 (2016) 16126.
[99] X. Li et al., Joule 2 (7) (2018) 1331.
[100] Y. Zhang et al., Nano Energy 65 (2019) 104006.
[101] L. Zong et al., Nano Energy 50 (2018) 308.
[102] F.L. Meng et al., Adv. Funct. Mater. 30 (32) (2020) 2002867.
[103] P. Yang et al., Energ. Environ. Sci. 10 (9) (1923) 2017.
[104] P. Xiao et al., Nano Energy 68 (2020).
[105] L. Zhu et al., Adv. Energy Mater. 8 (16) (2018) 1702149.
[106] H. Zou et al., Nat. Commun. 10 (1) (2019).
[107] J.W. Post et al., J. Membr. Sci. 288 (1–2) (2007) 218.
[108] G. Xue et al., Nat. Nanotechnol. 12 (4) (2017) 317.
[109] T. Ding et al., Chin. Sci. Bull. 63 (27) (2018) 2846.
[110] L. Cui et al., Adv. Mater. 30 (22) (2018) e1706805.
[111] W. Wang et al., Nat. Commun. 10 (1) (2019) 3012.
[112] N. Xu et al., Joule 4 (2) (2020) 347.
[113] R. Li et al., Nat. Sustain. (2020).
[114] J. Lao et al., Nano Energy 70 (2020).
[115] T. Ding et al., Adv. Funct. Mater. 27 (2017) 22.
[116] J. Li et al., Nano Energy 58 (2019) 797.
[117] J. Sun et al., Nano Energy 57 (2019) 269.
[118] N. Zhang et al., ACS Appl Energ. Mater. 2 (8) (2019) 6060.
[119] B. Hou et al., Carbon 140 (2018) 488.
[120] M.-Q. Yang et al., Adv. Funct. Mater. (2020).
[121] Y. Zhou et al., Nano Energy 77 (2020) 105102.
[122] M. Oelgemoller, Chem. Rev. 116 (17) (2016) 9664.
[123] G. Chen et al., Angew. Chem. Int. Ed. Engl. 58 (49) (2019) 17528.
[124] Y.J. Kim et al., Aust. J. Chem. 68 (11) (2015) 1653.
[125] D. Spasiano et al., Appl. Catal. B 136–137 (2013) 56.
[126] D. Dondi et al., Green Chem. 11 (10) (2009) 1653.
[127] M. Fischer, Angew. Chem., Int. Ed. Engl. 17 (1) (1978) 16.
[128] C. Finnerty et al., Environ. Sci. Technol. 51 (20) (2017) 11701.
[129] Z. Liu et al., Glob Chall 1 (2) (2017) 1600003.
[130] X. Li et al., Proc. Natl. Acad. Sci. USA 113 (49) (2016) 13953.
[131] L. Noureen et al., ACS Appl. Mater. Interfaces 12 (5) (2020) 6343.
[132] J. Huang et al., Energy Convers. Manage. 132 (2017) 452.
[133] X. Wang et al., Energy Convers. Manage. 173 (2018) 158.
[134] C. Zhang et al., Energy Technol. 7 (11) (2019).
[135] Y. Xu et al., J. Mater. Chem. A 7 (39) (2019) 22296.
[136] C. Chen et al., Nano Energy 51 (2018) 451.
[137] M.-Q. Yang et al., Angew. Chem. Int. Ed. 58 (10) (2019) 3077.
[138] D. Hao et al., ACS Sustainable Chem. Eng. 6 (8) (2018) 10789.
[139] B. Allegranzi et al., Lancet 377 (9761) (2011) 228.
[140] D. Pittet, L. Donaldson, Infect. Control. Hosp. Epidemiol. 26 (11) (2005) 891.
[141] D. Pittet et al., J. Hosp. Infect. 68 (4) (2008) 285.
[142] Y. Zhang et al., Nanoscale 9 (48) (2017) 19384.
[143] J. Li et al., Adv. Mater. 30 (49) (2018) e1805159.
[144] C. Chang et al., ACS Appl. Mater. Interfaces 11 (20) (2019) 18466.